Perturbative, Post-Newtonian, and General Relativistic Dynamics of Black Hole Binaries

Alexandre Le Tiec

University of Maryland

Based on collaborations with L. Barack, L. Blanchet, A. Buonanno, S. Detweiler, A. Mroué, H. Pfeiffer, N. Sago, A. Taracchini, B. Whiting

● = PN, ● = SF, ● = NR, ● = EOB

Outline

1. Modelling the relativistic dynamics of black hole binaries
2. Periastron advance in binary black holes
3. Redshift observable for circular orbits
4. Redshift observable for eccentric orbits

Outline

Interferometric detectors of gravitational waves (GW)

Virgo (Cascina, Italy)

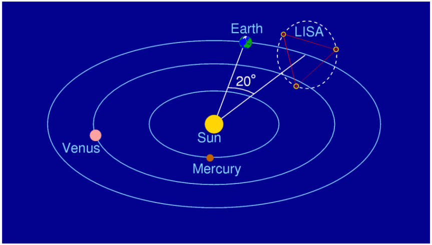

LISA (design)

High frequency band:
$10\ \text{Hz} \lesssim f \lesssim 10^3\ \text{Hz}$

Low frequency band:
$10^{-4}\ \text{Hz} \lesssim f \lesssim 10^{-1}\ \text{Hz}$

Main sources of GW for Virgo/LIGO and LISA

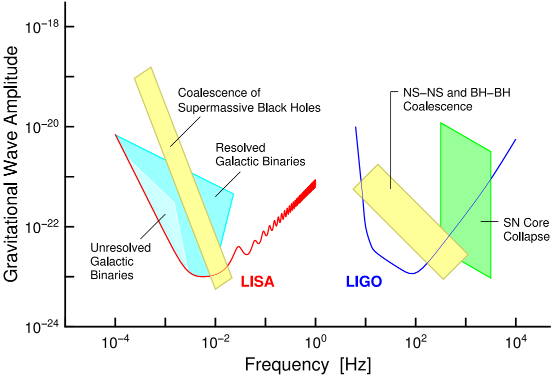

- Binary neutron stars ($M \sim 1.4 M_\odot$)
- Stellar mass black hole binaries ($M \sim 10 M_\odot$)
- Supermassive black hole binaries ($M \sim 10^6 M_\odot$)
- Extreme mass ratio inspirals (EMRIs)

Methods to model the dynamics of BH binaries

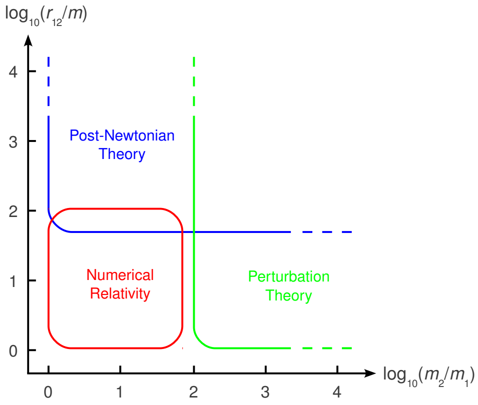

Methods to model the dynamics of BH binaries

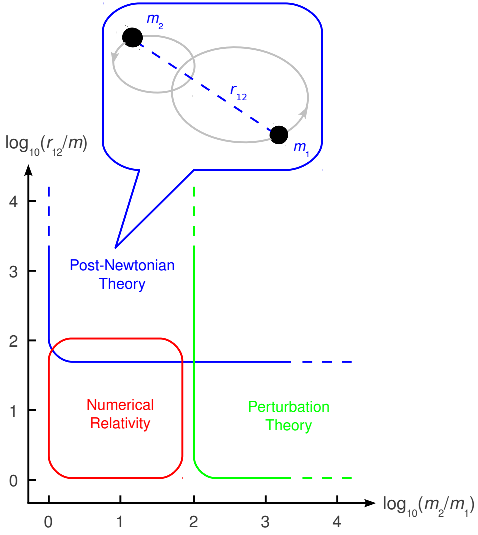

Methods to model the dynamics of BH binaries

The post-Newtonian formalism

Perturbation parameter

$$\varepsilon_{\text{PN}} \sim \frac{{v_{12}}^2}{c^2} \sim \frac{Gm}{r_{12}c^2} \ll 1$$

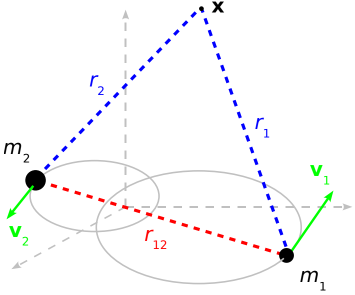

Example

$$g_{00}(\mathbf{x}) = -1 + \underbrace{\frac{2Gm_1}{r_1 c^2}}_{\text{Newtonian}} + \underbrace{\frac{4Gm_2 {v_2}^2}{r_2 c^4}}_{\text{1PN term}} + \cdots + (1 \leftrightarrow 2)$$

Methods to model the dynamics of BH binaries

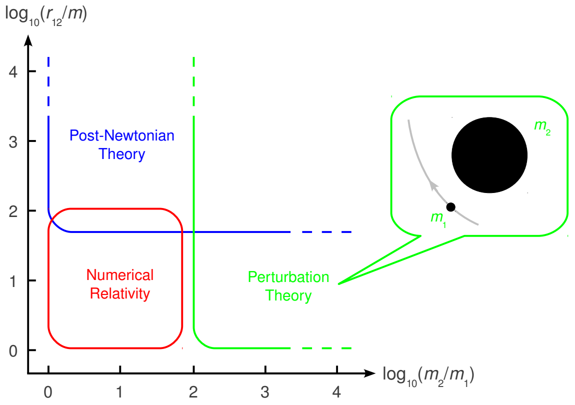

Methods to model the dynamics of BH binaries

Black hole perturbation theory and the gravitational self-force

Spacetime metric

$$g_{\mu\nu} = \bar{g}_{\mu\nu}$$

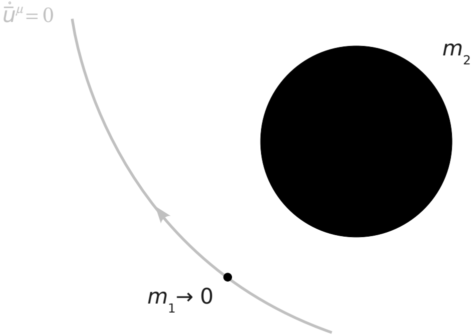

Methods to model the dynamics of BH binaries

Black hole perturbation theory and the gravitational self-force

Spacetime metric

$$g_{\mu\nu} = \bar{g}_{\mu\nu}$$

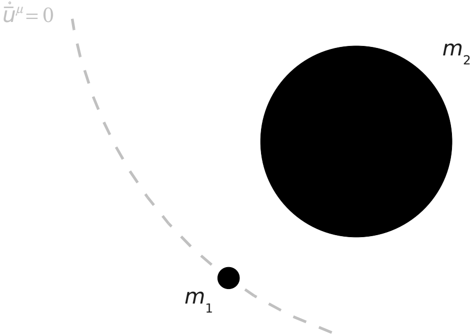

Perturbation parameter

$$q \equiv \frac{m_1}{m_2} \ll 1$$

Methods to model the dynamics of BH binaries

Black hole perturbation theory and the gravitational self-force

Spacetime metric

$$g_{\mu\nu} = \bar{g}_{\mu\nu} + h_{\mu\nu}$$

Perturbation parameter

$$q \equiv \frac{m_1}{m_2} \ll 1$$

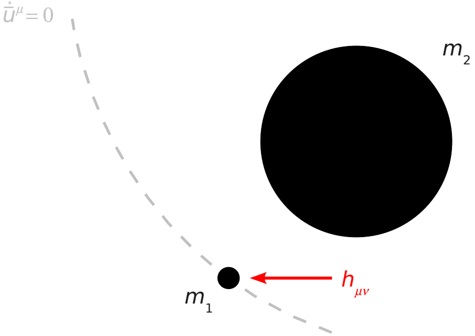

Methods to model the dynamics of BH binaries

Black hole perturbation theory and the gravitational self-force

Spacetime metric

$$g_{\mu\nu} = \bar{g}_{\mu\nu} + h_{\mu\nu}$$

Perturbation parameter

$$q \equiv \frac{m_1}{m_2} \ll 1$$

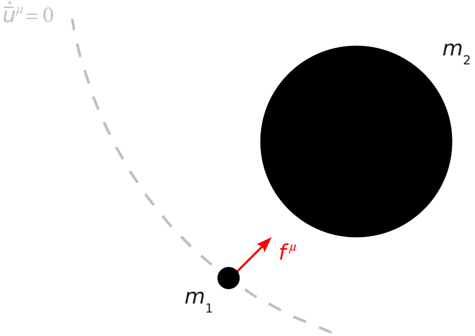

Methods to model the dynamics of BH binaries

Black hole perturbation theory and the gravitational self-force

Spacetime metric

$$g_{\mu\nu} = \bar{g}_{\mu\nu} + h_{\mu\nu}$$

Perturbation parameter

$$q \equiv \frac{m_1}{m_2} \ll 1$$

Self-force (SF) effect

$$\dot{\bar{u}}^\mu = f^\mu = \mathcal{O}(q)$$

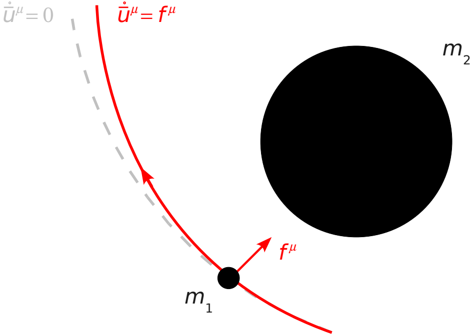

Methods to model the dynamics of BH binaries

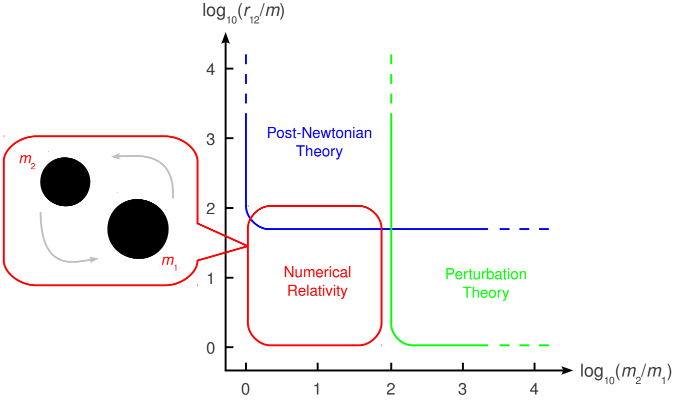

Methods to model the dynamics of BH binaries

Numerical relativity

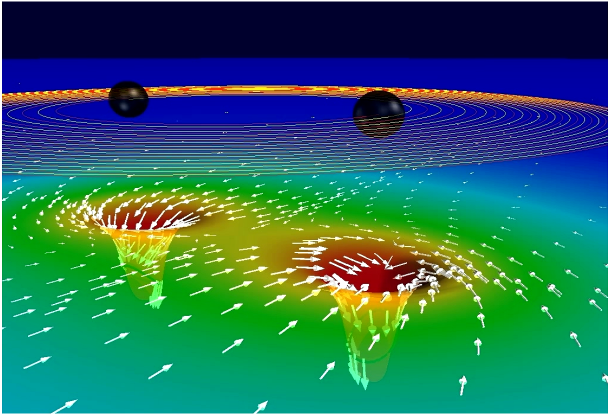

[Caltech-Cornell collaboration, *Spectral Einstein Code*]

Methods to model the dynamics of BH binaries

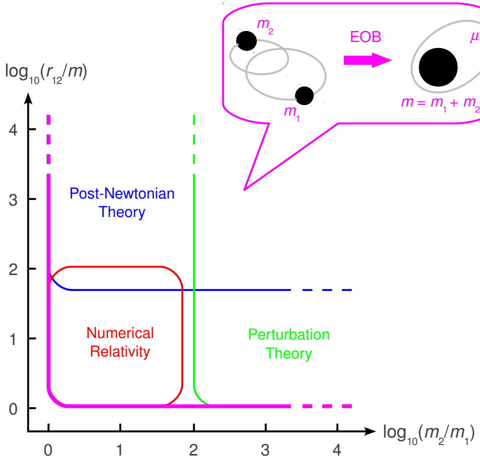

Methods to model the dynamics of BH binaries

Effective-one-body method

- Motion of a test-particle of mass $\mu = m_1 m_2 / m$ in a static and spherically symmetric effective metric

$$\mathrm{d}s^2_{\text{eff}} = -A(r;\nu)\,\mathrm{d}t^2 + B(r;\nu)\,\mathrm{d}r^2 + r^2\left(\mathrm{d}\theta^2 + \sin^2\theta\,\mathrm{d}\varphi^2\right)$$

- Reduces to the Schwarzschild metric of a black hole of mass $m = m_1 + m_2$ in the limit $\nu \to 0$
- Potentials determined so as to recover the 3PN dynamics:

$$A = 1 - 2u + 2\nu u^3 + \left(\frac{94}{3} - \frac{41}{32}\pi^2\right)\nu u^4 + \mathcal{O}(u^5)$$
$$\bar{D} = 1 + 6\nu u^2 + (52 - 6\nu)\,\nu u^3 + \mathcal{O}(u^4)$$

where $\bar{D} \equiv (AB)^{-1}$ and $u \equiv m/r$

Comparing the predictions from these methods

Why?

- Cross-check the validity of the various calculations

Comparing the predictions from these methods

Why?

- Cross-check the validity of the various calculations
- Determine domains of validity of approximation schemes

Comparing the predictions from these methods

Why?

- Cross-check the validity of the various calculations
- Determine domains of validity of approximation schemes
- Test some technically simplifying assumptions (e.g. use of point particles + regularization)

Comparing the predictions from these methods

Why?

- Cross-check the validity of the various calculations
- Determine domains of validity of approximation schemes
- Test some technically simplifying assumptions
  (e.g. use of point particles + regularization)
- Extract previously unknown information
  (e.g. determination of high-order PN coefficients)

Comparing the predictions from these methods

Why?

- Cross-check the validity of the various calculations
- Determine domains of validity of approximation schemes
- Test some technically simplifying assumptions
  (e.g. use of point particles + regularization)
- Extract previously unknown information
  (e.g. determination of high-order PN coefficients)
- Improve GW templates for coalescing compact binaries

Comparing the predictions from these methods

Why?

- Cross-check the validity of the various calculations
- Determine domains of validity of approximation schemes
- Test some technically simplifying assumptions
  (e.g. use of point particles + regularization)
- Extract previously unknown information
  (e.g. determination of high-order PN coefficients)
- Improve GW templates for coalescing compact binaries

How?

✘ Use the same coordinate system in all calculations

Comparing the predictions from these methods

Why?

- Cross-check the validity of the various calculations
- Determine domains of validity of approximation schemes
- Test some technically simplifying assumptions
(e.g. use of point particles + regularization)
- Extract previously unknown information
(e.g. determination of high-order PN coefficients)
- Improve GW templates for coalescing compact binaries

How?

✘ Use the same coordinate system in all calculations

✔ Use coordinate invariant relations to avoid gauge ambiguities

Outline

Relativistic precession of Mercury's perihelion

- Observed anomalous precession of Mercury's perihelion of $\sim 43''/\text{century}$

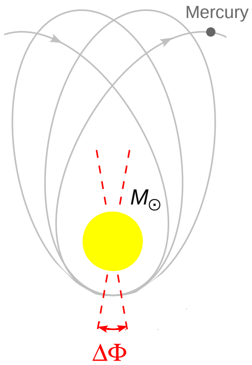

Relativistic precession of Mercury's perihelion

- Observed anomalous precession of Mercury's perihelion of $\sim 43''/\text{century}$
- Accounted for by the leading order relativisic angular advance per orbit

$$\Delta\Phi_{\text{GR}} = \frac{6\pi G M_\odot}{c^2 a\,(1-e^2)}$$

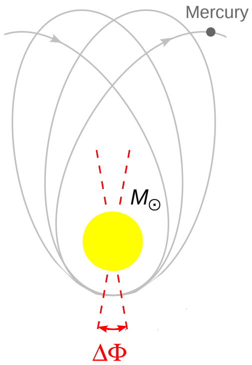

Relativistic precession of Mercury's perihelion

- Observed anomalous precession of Mercury's perihelion of $\sim 43''/\text{century}$
- Accounted for by the leading order relativisic angular advance per orbit

$$\Delta\Phi_{\text{GR}} = \frac{6\pi G M_\odot}{c^2 a\,(1 - e^2)}$$

- One of the first successes of Einstein's theory of general relativity

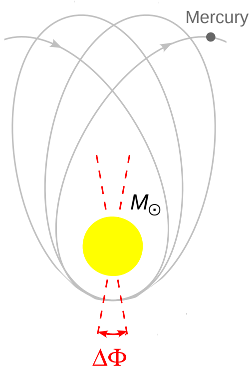

Relativistic precession of Mercury's perihelion

- Observed anomalous precession of Mercury's perihelion of $\sim 43'' /\text{century}$
- Accounted for by the leading order relativisic angular advance per orbit

$$\Delta\Phi_{\rm GR} = \frac{6\pi G M_\odot}{c^2 a\,(1-e^2)}$$

- One of the first successes of Einstein's theory of general relativity
- Relativisic periastron advance of $\sim {}^\circ/\text{year}$ now measured in binary pulsars

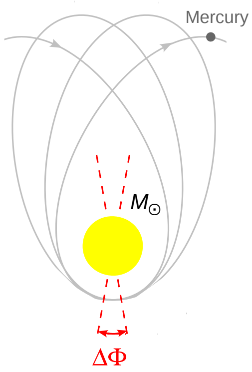

Periastron advance in black hole binaries

- Conservative part of the dynamics only
- Generic non-circular orbit parametrized by two frequencies:

$$\Omega_r = \frac{2\pi}{P}\,, \quad \Omega_\varphi = \frac{1}{P}\int_0^P \dot{\varphi}(t)\,\mathrm{d}t$$

- Periastron advance per orbital revolution

$$K \equiv \frac{\Omega_\varphi}{\Omega_r} = 1 + \frac{\Delta\Phi}{2\pi}$$

- In the circular orbit limit $e \to 0$, the relation $K(\Omega_\varphi)$ is coordinate invariant

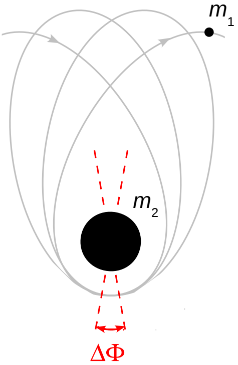

Analytical results for $K(\Omega_\varphi)$

- Third post-Newtonian result [Damour, Jaranowski & Schäfer 2000]

$$K = 1 + 3x + \left(\frac{27}{2} - 7\nu\right)x^2 + \Big(\cdots\Big)x^3 + \mathcal{O}(x^4)$$

where $\nu \equiv m_1 m_2/m^2$ and $x \equiv (m\Omega_\varphi)^{2/3} \sim v^2$

Analytical results for $K(\Omega_\varphi)$

- Third post-Newtonian result [Damour, Jaranowski & Schäfer 2000]

$$K = 1 + 3x + \left(\frac{27}{2} - 7\nu\right)x^2 + \left(\cdots\right)x^3 + \mathcal{O}(x^4)$$

where $\nu \equiv m_1 m_2 / m^2$ and $x \equiv (m\Omega_\varphi)^{2/3} \sim v^2$

- Gravitational self-force result [Barack & Sago 2010]

$$K = \frac{1}{\sqrt{1-6x}} + \underbrace{q\, K_{\text{SF}}(x)}_{\text{SF effect}} + \mathcal{O}(q^2)$$

where $q \equiv m_1 / m_2$.

Analytical results for $K(\Omega_\varphi)$

- Third post-Newtonian result [Damour, Jaranowski & Schäfer 2000]

$$K = 1 + 3x + \left(\frac{27}{2} - 7\nu\right)x^2 + \left(\cdots\right)x^3 + \mathcal{O}(x^4)$$

where $\nu \equiv m_1 m_2/m^2$ and $x \equiv (m\Omega_\varphi)^{2/3} \sim v^2$

- Gravitational self-force result [Barack & Sago 2010]

$$K = \frac{1}{\sqrt{1-6x}} + \underbrace{q\, K_{\rm SF}(x)}_{\text{SF effect}} + \mathcal{O}(q^2)$$

where $q \equiv m_1/m_2$. Since $q = \nu + \mathcal{O}(\nu^2)$, we also have

$$K = \frac{1}{\sqrt{1-6x}} + \nu\, K_{\rm SF}(x) + \mathcal{O}(\nu^2)$$

Analytical results for $K(\Omega_\varphi)$

- Third post-Newtonian result [Damour, Jaranowski & Schäfer 2000]

$$K = 1 + 3x + \left(\frac{27}{2} - 7\nu\right)x^2 + \left(\cdots\right)x^3 + \mathcal{O}(x^4)$$

where $\nu \equiv m_1 m_2/m^2$ and $x \equiv (m\Omega_\varphi)^{2/3} \sim v^2$

- Gravitational self-force result [Barack & Sago 2010]

$$K = \frac{1}{\sqrt{1-6x}} + \underbrace{q\, K_{\text{SF}}(x)}_{\text{SF effect}} + \mathcal{O}(q^2)$$

where $q \equiv m_1/m_2$. Since $q = \nu + \mathcal{O}(\nu^2)$, we also have

$$K = \frac{1}{\sqrt{1-6x}} + \nu\, K_{\text{SF}}(x) + \mathcal{O}(\nu^2)$$

- Effective-one-body result [Buonanno & Damour 1999; Damour 2010]

Early numerical results for $K(\Omega_\varphi)$

[Mroué, Pfeiffer, Kidder & Teukolsky 2010]

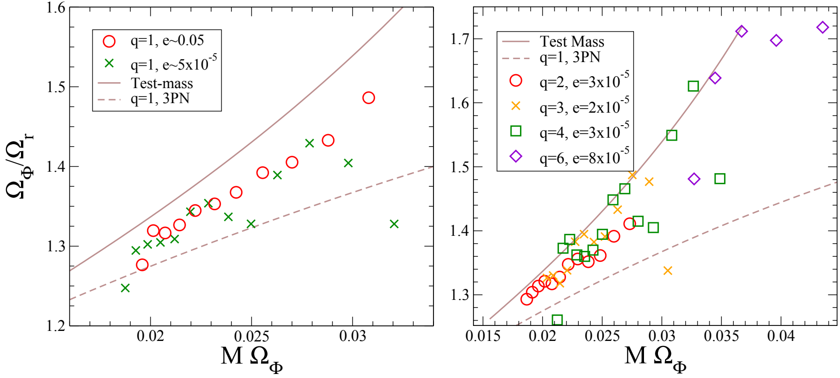

Comparison for mass ratio 1:1

[Le Tiec, Mroué, Barack, Buonanno, Pfeiffer, Sago & Taracchini (in preparation)]

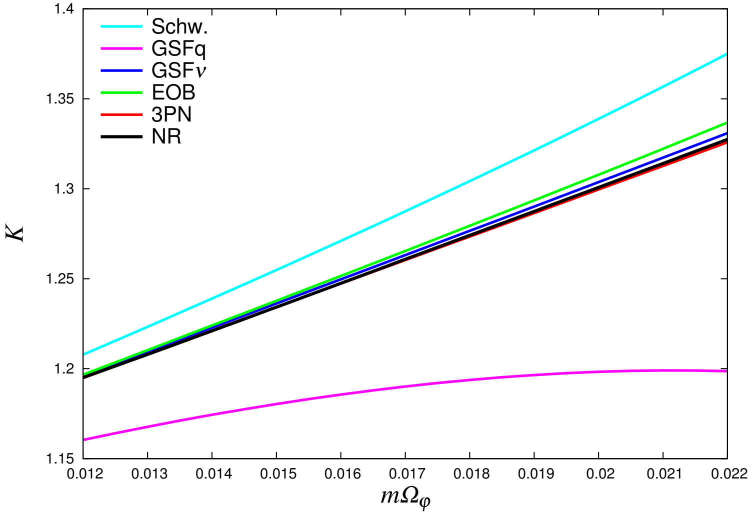

Comparison for mass ratio 1:8

[Le Tiec, Mroué, Barack, Buonanno, Pfeiffer, Sago & Taracchini (in preparation)]

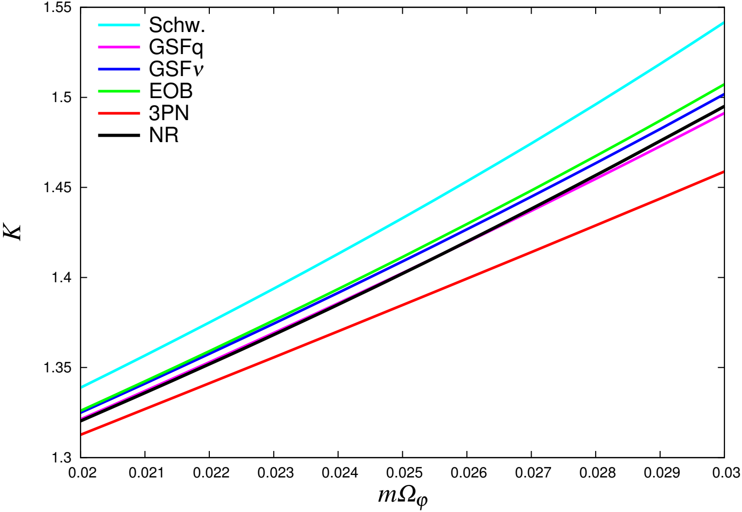

Outline

Common domain of validity of PN and SF calculations

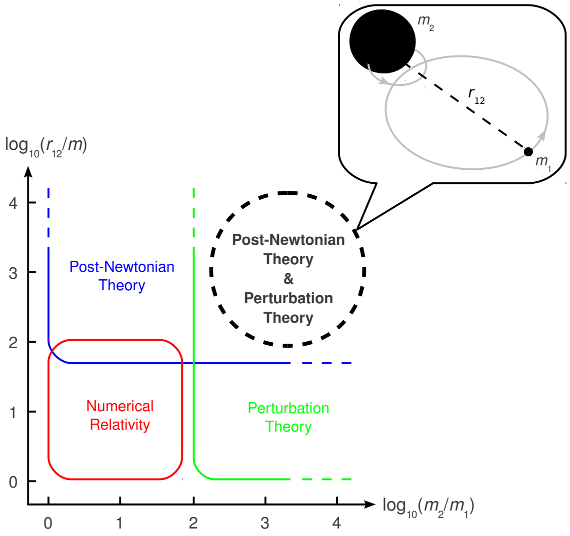

The "redshift observable" for circular orbits

- Conservative part of the dynamics only
- For circular orbits, the geometry admits an helical Killing vector k^α such that

$$k^\alpha = (\partial_t)^\alpha + \Omega_\varphi \, (\partial_\varphi)^\alpha \quad \text{(asymptotically)}$$

- Four-velocity u^α of the particle necessarily tangent to the helical Killing vector:

$$u^\alpha = u^T k_1^\alpha$$

- Relation $u^T(\Omega_\varphi)$ well defined in PN and SF frameworks, and coordinate invariant

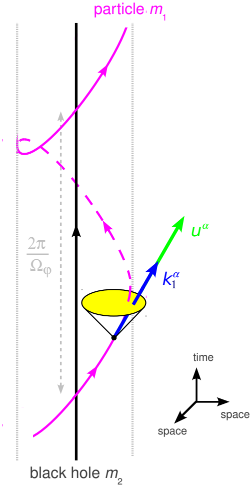

Physical interpretations of the quantity u^T

- In a gauge such that $k^\alpha \partial_\alpha = \partial_t + \Omega_\varphi \, \partial_\varphi$ everywhere, u^T is the time component of the particle's four-velocity:

$$u^T = u^t$$

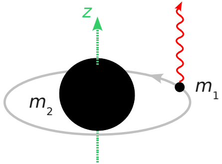

- It measures the redshift of light rays emitted from the particle, and reaching $\mathcal{I}^+$ along the rotation axis [Detweiler 08]

$$\frac{\mathcal{E}_{\text{obs}}}{\mathcal{E}_{\text{em}}} \equiv \frac{(u^\alpha_{\text{obs}} \nu_\alpha)_B}{(u^\alpha_{\text{em}} \nu_\alpha)_A} = \frac{1}{u^t}$$

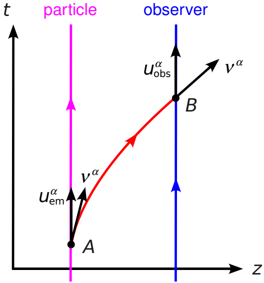

Post-Newtonian result for the SF effect on $u^t(\Omega_\varphi)$

[Blanchet, Detweiler, Le Tiec & Whiting 2010 (a,b)]

- In the extreme mass ratio limit $q \ll 1$:

$$u^t = \frac{1}{\sqrt{1-3y}} \underbrace{- q\, u^t_{\text{SF}}(y)}_{\text{SF effect}} + \mathcal{O}(q^2)$$

- PN result expressed as a power series in $y \equiv (m_2 \Omega_\varphi)^{2/3} \sim v^2$:

$$u^t_{\text{SF}} = y + 2y^2 + 5y^3 + \overbrace{\left(\frac{121}{3} - \frac{41}{32}\pi^2\right) y^4}^{\text{3PN contribution}} + \left(a_4 + \underbrace{\frac{64}{5}\ln y}_{\text{4PN log}}\right) y^5 + \left(a_5 \underbrace{- \frac{956}{105}\ln y}_{\text{5PN log}}\right) y^6 + o(y^6)$$

- The 4PN and 5PN polynomial coefficients $\{a_4, a_5\}$ are unknown, but can be extracted from the SF calculation

High-precision comparison of the 3PN coefficient

- We fit the result of the SF calculation by a PN series

$$u^t_{\mathrm{SF}} = \sum_{n\geqslant 0} a_n\, y^{n+1} + \ln y \sum_{n\geqslant 4} b_n\, y^{n+1}$$

High-precision comparison of the 3PN coefficient

- We fit the result of the SF calculation by a PN series

$$u^t_{\mathrm{SF}} = \sum_{n\geqslant 0} a_n\, y^{n+1} + \ln y \sum_{n\geqslant 4} b_n\, y^{n+1}$$

- The known values of the coeffs. $\{a_0, a_1, a_2\}$ up to 2PN are used, as well as the 4PN and 5PN logarithmic coeffs. $\{b_4, b_5\}$

High-precision comparison of the 3PN coefficient

- We fit the result of the SF calculation by a PN series

$$u^t_{\mathrm{SF}} = \sum_{n\geqslant 0} a_n\, y^{n+1} + \ln y \sum_{n\geqslant 4} b_n\, y^{n+1}$$

- The known values of the coeffs. $\{a_0, a_1, a_2\}$ up to 2PN are used, as well as the 4PN and 5PN logarithmic coeffs. $\{b_4, b_5\}$
- The fit of the numerical SF data yields for the 3PN coefficient

$$a_3^{\mathrm{SF}} = 27.6879034 \pm 0.0000004$$

High-precision comparison of the 3PN coefficient

- We fit the result of the SF calculation by a PN series

$$u^t_{\mathrm{SF}} = \sum_{n\geqslant 0} a_n\, y^{n+1} + \ln y \sum_{n\geqslant 4} b_n\, y^{n+1}$$

- The known values of the coeffs. $\{a_0, a_1, a_2\}$ up to 2PN are used, as well as the 4PN and 5PN logarithmic coeffs. $\{b_4, b_5\}$
- The fit of the numerical SF data yields for the 3PN coefficient

$$a_3^{\mathrm{SF}} = 27.6879034 \pm 0.0000004$$

- To be compared with the exact analytical result

$$a_3 = \frac{121}{3} - \frac{41}{32}\pi^2 = 27.6879026\cdots$$

High-precision comparison of the 3PN coefficient

- We fit the result of the SF calculation by a PN series

$$u^t_{\mathrm{SF}} = \sum_{n\geqslant 0} a_n\, y^{n+1} + \ln y \sum_{n\geqslant 4} b_n\, y^{n+1}$$

- The known values of the coeffs. $\{a_0, a_1, a_2\}$ up to 2PN are used, as well as the 4PN and 5PN logarithmic coeffs. $\{b_4, b_5\}$
- The fit of the numerical SF data yields for the 3PN coefficient

$$a_3^{\mathrm{SF}} = 27.6879034 \pm 0.0000004$$

- To be compared with the exact analytical result

$$a_3 = \frac{121}{3} - \frac{41}{32}\pi^2 = 27.6879026\cdots$$

- The two calculations are therefore in agreement at the 2σ level with 9 significant digits

High-order PN fit of the gravitational SF calculation

- We fit the result of the SF calculation by a PN series

$$u^t_{\mathrm{SF}} = \sum_{n\geqslant 0} a_n\, y^{n+1} + \ln y \sum_{n\geqslant 4} b_n\, y^{n+1}$$

- We also include the know value of the 3PN coefficient a_3
- Our best fit yields:

PN order	Coeff.	Value
4	a_4	$+114.34747(5)$
5	a_5	$+245.53(1)$
6	a_6	$+695(2)$
6	b_6	$-339.3(5)$
7	a_7	$+5837(16)$

Comparison of the PN and SF results

[Blanchet, Detweiler, Le Tiec & Whiting 2010 (a,b)]

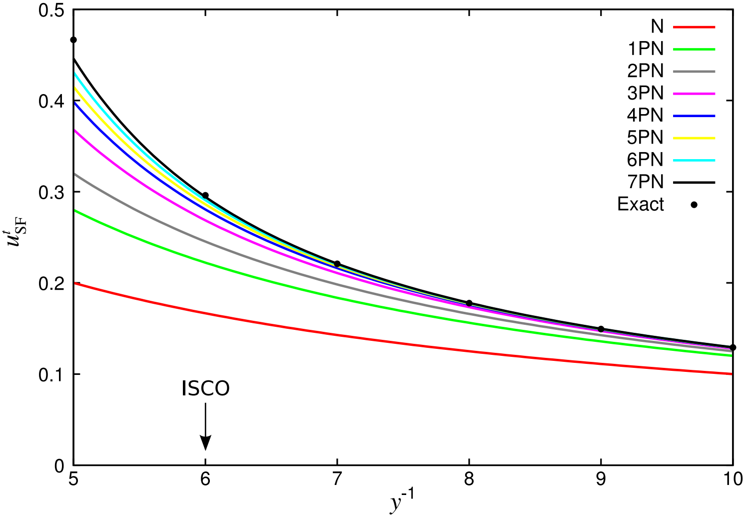

Outline

Proper time-averaged redshift observable

- Conservative part of the dynamics only

Proper time-averaged redshift observable

- Conservative part of the dynamics only
- Averaging w.r.t. proper time τ over one radial period:

$$\langle u^t \rangle_\tau \equiv \frac{1}{T} \int_0^T u^t(\tau)\, \mathrm{d}\tau = \frac{P}{T}$$

Proper time-averaged redshift observable

- Conservative part of the dynamics only
- Averaging w.r.t. proper time τ over one radial period:

$$\langle u^t \rangle_\tau \equiv \frac{1}{T} \int_0^T u^t(\tau)\,\mathrm{d}\tau = \frac{P}{T}$$

- The relation $\langle u^t \rangle_\tau(\Omega_r, \Omega_\varphi)$ is coordinate invariant

Proper time-averaged redshift observable

- Conservative part of the dynamics only
- Averaging w.r.t. proper time τ over one radial period:

$$\langle u^t \rangle_\tau \equiv \frac{1}{T} \int_0^T u^t(\tau)\,\mathrm{d}\tau = \frac{P}{T}$$

- The relation $\langle u^t \rangle_\tau(\Omega_r, \Omega_\varphi)$ is coordinate invariant
- Making use of the quasi-Keplerian parametrization of the motion, the 1PN-accurate result reads

$$\langle u^t \rangle_\tau = 1 + \left(\frac{3}{4} + \frac{3}{4}\Delta - \frac{\nu}{2} \right) x + \left(\frac{3}{16} + \frac{3}{16}\Delta - \frac{7}{2}\nu - \frac{5}{8}\Delta\,\nu + \frac{\nu^2}{24} + \frac{3+3\Delta}{\sqrt{\iota}} - \frac{3+3\Delta-2\nu}{2\iota} \right) x^2 + \mathcal{O}(x^3)$$

where $\Delta \equiv \sqrt{1-4\nu}$ and $\iota \equiv 3x/(K-1) \sim 1 - e^2$

PN result for the SF effect on $\langle u^t \rangle_\tau(\Omega_r, \Omega_\varphi)$

- In the extreme mass ratio limit $q \ll 1$:

$$\langle u^t \rangle_\tau = \langle u^t \rangle_\tau^{\text{Schw}} + \underbrace{q \, \langle u^t \rangle_\tau^{\text{SF}}}_{\text{SF effect}} + \mathcal{O}(q^2)$$

- The 1PN-accurate result reads

$$\langle u^t \rangle_\tau^{\text{SF}} = y + \left(4 - \frac{2}{\sqrt{\lambda}}\right) y^2 + \mathcal{O}(y^3)$$

where $\lambda \equiv 3y/(K-1) \sim 1 - e^2$

- Alternatively, the result can be parametrized in terms of some coordinate dependant semi-latus rectum p and eccentricity e

Comparison of the PN and SF results

[Barack, Le Tiec & Sago (in progress)]

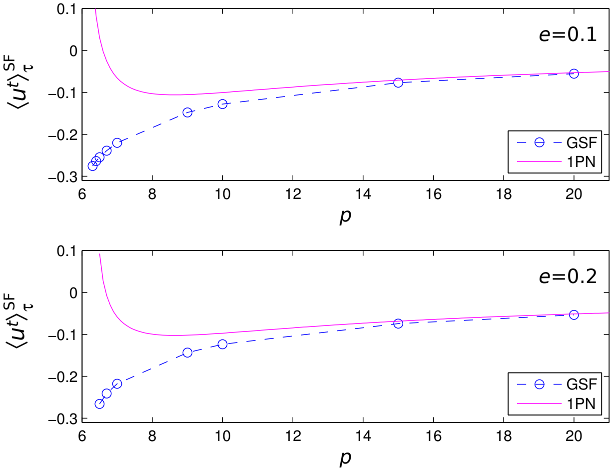

Comparison of the PN and SF results

[Barack, Le Tiec & Sago (in progress)]

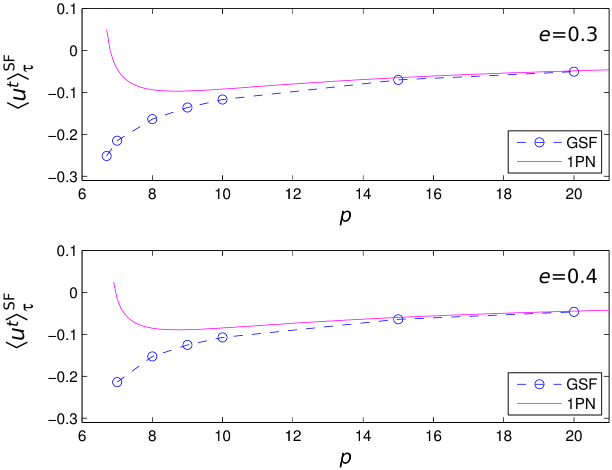

Coordinate time-averaged redshift observable

- Averaging w.r.t. coordinate time t over one radial period:

$$\langle u^t \rangle_t \equiv \frac{1}{P} \int_0^P u^t(t)\,\mathrm{d}t$$

- The relation $\langle u^t \rangle_t(\Omega_r, \Omega_\varphi)$ is likely *not* coordinate invariant
- In the extreme mass ratio limit $q \ll 1$:

$$\langle u^t \rangle_t = \langle u^t \rangle_t^{\text{Schw}} + \underbrace{q\,\langle u^t \rangle_t^{\text{SF}}}_{\text{SF effect}} + \mathcal{O}(q^2)$$

- Relation $\langle u^t \rangle_t^{\text{SF}}(\Omega_r, \Omega_\varphi)$ computed exactly within the SF formalism, and at 1PN order in post-Newtonian theory

Comparison of the PN and SF results

[Barack, Le Tiec & Sago (in progress)]

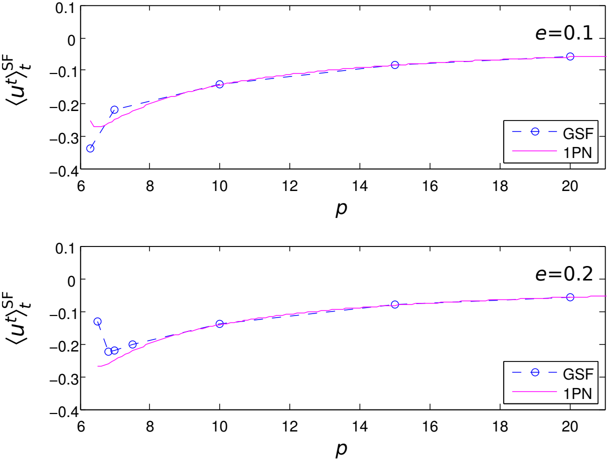

Comparison of the PN and SF results

[Barack, Le Tiec & Sago (in progress)]

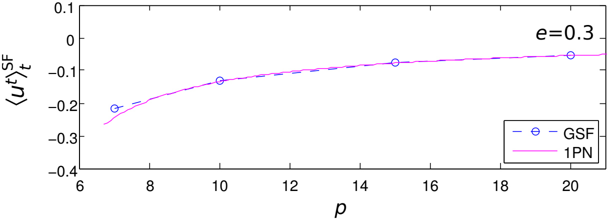

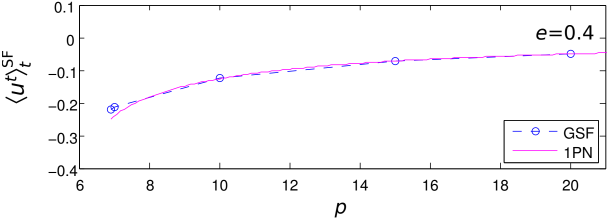

Summary

- The dynamics of BH binaries can be investigated using a variety of approximation schemes and numerical techniques

Summary

- The dynamics of BH binaries can be investigated using a variety of approximation schemes and numerical techniques
- All these methods are now mature enough to produce some physically meaningful (i.e. coordinate invariant) results

Summary

- The dynamics of BH binaries can be investigated using a variety of approximation schemes and numerical techniques
- All these methods are now mature enough to produce some physically meaningful (i.e. coordinate invariant) results
- By comparing these results, we can:

Summary

- The dynamics of BH binaries can be investigated using a variety of approximation schemes and numerical techniques
- All these methods are now mature enough to produce some physically meaningful (i.e. coordinate invariant) results
- By comparing these results, we can:
    - Cross-check the validity of the various calculations
      ↳ e.g. GSF vs 1PN results for $\langle u^t \rangle_\tau^{\mathrm{SF}}(\Omega_r, \Omega_\varphi)$

Summary

- The dynamics of BH binaries can be investigated using a variety of approximation schemes and numerical techniques
- All these methods are now mature enough to produce some physically meaningful (i.e. coordinate invariant) results
- By comparing these results, we can:
  - Cross-check the validity of the various calculations
    ↳ e.g. GSF vs 1PN results for $\langle u^t \rangle_\tau^{\mathrm{SF}}(\Omega_r, \Omega_\varphi)$
  - Determine domains of validity of approximation methods
    ↳ e.g. PN/SF vs NR results for $K(\Omega_\varphi)$

Summary

- The dynamics of BH binaries can be investigated using a variety of approximation schemes and numerical techniques
- All these methods are now mature enough to produce some physically meaningful (i.e. coordinate invariant) results
- By comparing these results, we can:
  - Cross-check the validity of the various calculations
    ↳ e.g. GSF vs 1PN results for $\langle u^t \rangle_\tau^{\mathrm{SF}}(\Omega_r, \Omega_\varphi)$
  - Determine domains of validity of approximation methods
    ↳ e.g. PN/SF vs NR results for $K(\Omega_\varphi)$
  - Test some technically simplifying assumptions
    ↳ e.g. agreement on 3PN coefficient in $u^t_{\mathrm{SF}}(\Omega_\varphi)$

Summary

- The dynamics of BH binaries can be investigated using a variety of approximation schemes and numerical techniques
- All these methods are now mature enough to produce some physically meaningful (i.e. coordinate invariant) results
- By comparing these results, we can:
  - Cross-check the validity of the various calculations
    ↳ e.g. GSF vs 1PN results for $\langle u^t \rangle_\tau^{\rm SF}(\Omega_r, \Omega_\varphi)$
  - Determine domains of validity of approximation methods
    ↳ e.g. PN/SF vs NR results for $K(\Omega_\varphi)$
  - Test some technically simplifying assumptions
    ↳ e.g. agreement on 3PN coefficient in $u^t_{\rm SF}(\Omega_\varphi)$
  - Extract previously unknown information
    ↳ e.g. high-order PN coefficients in $u^t_{\rm SF}(\Omega_\varphi)$

Summary

- The dynamics of BH binaries can be investigated using a variety of approximation schemes and numerical techniques
- All these methods are now mature enough to produce some physically meaningful (i.e. coordinate invariant) results
- By comparing these results, we can:
  - Cross-check the validity of the various calculations
    ↳ e.g. GSF vs 1PN results for $\langle u^t \rangle_\tau^{\mathrm{SF}}(\Omega_r, \Omega_\varphi)$
  - Determine domains of validity of approximation methods
    ↳ e.g. PN/SF vs NR results for $K(\Omega_\varphi)$
  - Test some technically simplifying assumptions
    ↳ e.g. agreement on 3PN coefficient in $u^t_{\mathrm{SF}}(\Omega_\varphi)$
  - Extract previously unknown information
    ↳ e.g. high-order PN coefficients in $u^t_{\mathrm{SF}}(\Omega_\varphi)$
  - Improve GW templates for coalescing compact binaries

EXTRA SLIDES

Post-Newtonian equations of motion for compact binaries

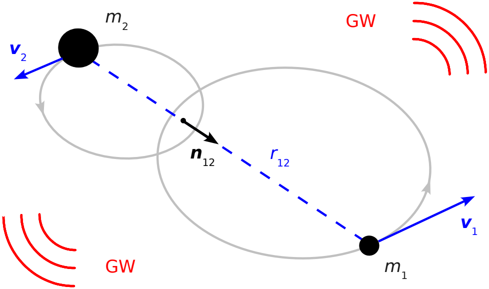

$$\frac{\mathrm{d}\mathbf{v}_1}{\mathrm{d}t} = \underbrace{-\frac{Gm_2}{r_{12}^2}\mathbf{n}_{12} + \frac{\mathbf{A}_{1PN}}{c^2} + \frac{\mathbf{A}_{2PN}}{c^4}}_{\text{conservative terms}} + \underbrace{\frac{\mathbf{A}_{2.5PN}}{c^5}}_{\text{rad. reac.}} + \underbrace{\frac{\mathbf{A}_{3PN}}{c^6}}_{\text{cons. term}} + \underbrace{\frac{\mathbf{A}_{3.5PN}}{c^7}}_{\text{rad. reac.}} + \cdots$$

Dimensional regularization: a simple example

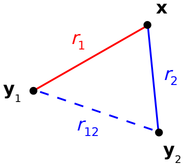

- Time component of the Newtonian metric in $d = 3$ space dimensions

$$g_{00}(\mathbf{x}) = -1 + \frac{2Gm_1}{c^2 r_1} + \frac{2Gm_2}{c^2 r_2} + \cdots$$

- Not defined at the location $\mathbf{y}_1$ in the limit $r_1 \to 0$
- Time component of the metric in d space dimensions

$$g_{00}^{(d)}(\mathbf{x}) = -1 + \frac{2G^{(d)}m_1}{c^2 r_1^{d-2}} + \frac{2G^{(d)}m_2}{c^2 r_2^{d-2}} + \cdots$$

- Analytic continuation in the space dimension: $d \in \mathbb{C}$
- Choose $\mathcal{R}(d) < 2$ such that $g_{00}^{(d)}$ is defined in the limit $r_1 \to 0$
- Relying on the uniqueness of analytic continuation, the 3-dimensional result is

$$g_{00}(\mathbf{y}_1) = \underset{d\to 3}{\mathrm{AC}}\left[\lim_{\mathbf{x}\to\mathbf{y}_1} g_{00}^{(d)}(\mathbf{x})\right] = -1 + \frac{2Gm_2}{c^2 r_{12}} + \cdots$$

Hereditary contributions originating from GW tails

- Gravitational radiation is scattered by the background curvature generated by the mass M of the source

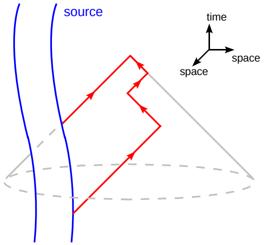

- Starting at 4N order, the near-zone metric depends on the entire past "history" of the source [Blanchet & Damour 1988]

$$\delta g_{00}^{\text{tail}}(x,t) = -\frac{8G^2 M}{5c^{10}} x^a x^b \int_{-\infty}^{t} \mathrm{d}t' \, M_{ab}^{(7)}(t') \ln\left(\frac{c(t-t')}{2r}\right)$$